Thermodynamics of Aminoglycoside−rRNA Recognition: The Binding of Neomycin-Class Aminoglycosides to the A Site of 16S rRNA†

Malvika Kaul‡ and Daniel S. Pilch*,‡,§

Department of Pharmacology, University of Medicine and Dentistry of New Jersey-Robert Wood Johnson Medical School, 675 Hoes Lane, Piscataway, New Jersey 08854-5635, and The Cancer Institute of New Jersey, New Brunswick, New Jersey, 08901

Received February 13, 2002; Revised Manuscript Received April 23, 2002

ABSTRACT: We use spectroscopic and calorimetric techniques to characterize the binding of the aminoglycoside antibiotics neomycin, paromomycin, and ribostamycin to a RNA oligonucleotide that models the A-site of *Escherichia coli* 16S rRNA. Our results reveal the following significant features: (i) Aminoglycoside binding enhances the thermal stability of the A-site RNA duplex, with the extent of this thermal enhancement decreasing with increasing pH and/or Na^+ concentration. (ii) The RNA binding enthalpies of the aminoglycosides become more exothermic (favorable) with increasing pH, an observation consistent with binding-linked protonation of one or more drug amino groups. (iii) Isothermal titration calorimetry (ITC) studies conducted as a function of buffer reveal that aminoglycoside binding to the host RNA is linked to the uptake of protons, with the number of linked protons being dependent on pH. Specifically, increasing the pH results in a corresponding increase in the number of linked protons. (iv) ITC studies conducted at 25 and 37 °C reveal that aminoglycoside−RNA complexation is associated with a negative heat capacity change (ΔC_p), the magnitude of which becomes greater with increasing pH. (v) The observed RNA binding affinities of the aminoglycosides decrease with increasing pH and/or Na^+ concentration. In addition, the thermodynamic forces underlying these RNA binding affinities also change as a function of pH. Specifically, with increasing pH, the enthalpic contribution to the observed RNA binding affinity increases, while the corresponding entropic contribution to binding decreases. (vi) The affinities of the aminoglycosides for the host RNA follow the hierarchy neomycin > paromomycin > ribostamycin. The enhanced affinity of neomycin relative to either paromomycin or ribostamycin is primarily, if not entirely, enthalpic in origin. (vii) The salt dependencies of the RNA binding affinities of neomycin and paromomycin are consistent with at least three drug NH_3^+ groups participating in electrostatic interactions with the host RNA. In the aggregate, our results reveal the impact of specific alterations in aminoglycoside structure on the thermodynamics of binding to an A-site model RNA oligonucleotide. Such systematic comparative studies are critical first steps toward establishing the thermodynamic database required for enhancing our understanding of the molecular forces that dictate and control aminoglycoside recognition of RNA.

Aminoglycosides are broad-spectrum antibiotics that are used most widely in the treatment of infections caused by aerobic gram-negative bacilli (*1*). The bactericidal activity of the aminoglycosides is derived from their ability to inhibit the translation process. They achieve this effect by binding to phylogenetically conserved sequences within the 16S ribosomal RNA ([1]rRNA) of the 30S ribosomal subunit (*2*, *3*), thereby inducing codon misreading as well as the inhibition of translocation (*4*, *5*).

Footprinting experiments have demonstrated that neomycin-class aminoglycosides target specific conserved sequences in the A-site of 16S rRNA (*2*, *3*). Neomycin-class aminoglycosides consist of one or more amino sugars linked to a six-carbon aminocyclitol (2-deoxystreptamine) at the 4,5-positions (Figure 1). The Puglisi group has used footprinting techniques to demonstrate that the binding site for neomycin-class aminoglycosides in the *Escherichia coli* 16S rRNA A-site of the 30S ribosomal subunit can be modeled by a 27-mer RNA oligonucleotide (*6*−*8*), whose sequence and secondary structure are depicted in Figure 2. NMR studies by the same group culminated in a solution structure of paromomycin in complex with the A-site RNA oligonucleotide (*6*, *8*). This structure, along with the corresponding structure of the drug-free RNA molecule, revealed several features worthy of note. First, the drug preferentially binds in the major groove of an asymmetric loop region in the host oligonucleotide, while forming an ensemble of hydrogen bonding and electrostatic contacts with the RNA. Second,

† This work was supported by grants from the American Cancer Society (RPG-99-153-01-C) and the New Jersey Commission on Cancer Research (00-64-CCR−S-0). D.S.P. was supported in part by a Young Investigator Award from The Cancer Institute of New Jersey.

* To whom correspondence should be addressed. Tel.: 732-235-3352. Fax: 732-235-4073. E-mail: pilchds@umdnj.edu.

‡ Department of Pharmacology, UMDNJ-Robert Wood Johnson Medical School.

§ The Cancer Institute of New Jersey.

[1] Abbreviations: rRNA, ribosomal RNA; ITC, isothermal titration calorimetry; DSC, differential scanning calorimetry; MES, 2-[N-Morpholino]ethanesulfonic acid; MOPS, 3-[N-Morpholino]propanesulfonic acid.

10.1021/bi020130f CCC: $22.00
Published on Web 05/22/2002

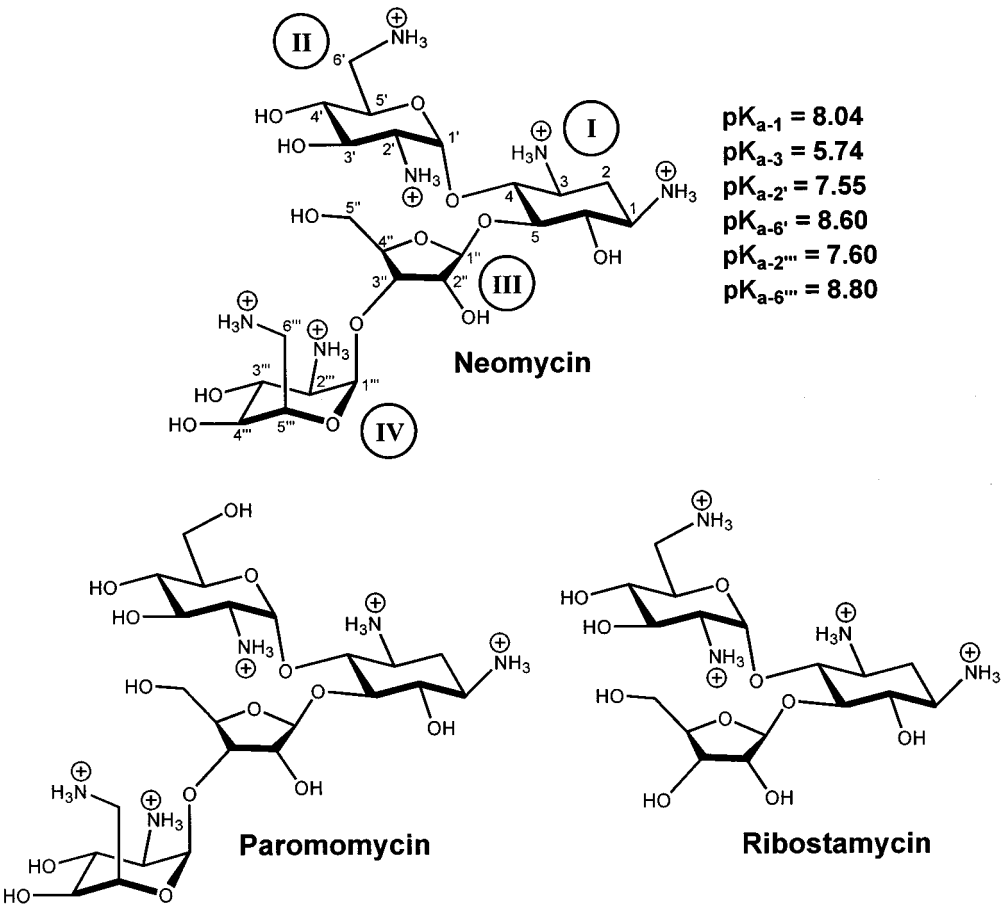

FIGURE 1: Structures of neomycin, paromomycin, and ribostamycin, with the atomic and ring numbering systems denoted in Arabic and Roman numerals, respectively. The NMR-derived (*15*) pK_a values for the six amino groups of neomycin are indicated.

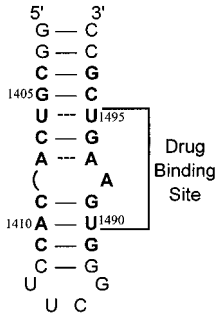

FIGURE 2: Secondary structure of the 27-mer A-site RNA oligonucleotide, as derived by NMR (*8*, *50*). Watson−Crick base pairs are denoted by solid lines, while mismatched base pairs are denoted by dashed lines. Bases present in *E. coli* 16S rRNA are depicted in bold face and are numbered as they are in 16S rRNA. The aminoglycoside binding site, as revealed by NMR and footprinting studies (*6*, *7*, *50*), is as indicated.

rings I and II of the drug appear to be required for the specific binding of neomycin-class aminoglycosides to rRNA. Third, the presence of the antibiotic causes the displacement of two adenine residues in the asymmetric loop (A1492 and A1493) toward the minor groove, thereby creating a binding pocket for the drug. This latter observation led to the proposal that aminoglycosides cause mistranslation by inducing a conformational change in the A-site of 16S rRNA that enhances its affinity for tRNA (*8*), a model for aminoglycoside-induced mistranslation that is consistent with kinetic studies indicating that neomycin-class aminoglycosides reduce the dissociation rate of tRNA from the ribosome, while also enhancing the initial binding reaction between the tRNA and the ribosome (*9*, *10*). Recent crystallographic and modeling studies by Ramakrishnan and co-workers on the 30S ribosomal subunit of *Thermus thermophilus* in complex with paromomycin lend further support to this model for aminoglycoside-induced mistranslation by revealing that the two adenine residues (A1492 and A1493) displaced by the bound drug can interact favorably with the minor groove of the codon-anticodon duplex and may thus stabilize the complex formed between this duplex and the ribosome, even with a noncognate tRNA (*11*).

This impressive structural picture of aminoglycoside−rRNA interactions needs to be complemented by energetic data, including dissection of the binding free energies into their enthalpic and entropic contributions. Such thermodynamic data on families of aminoglycoside−RNA complexes are critical for understanding the nature and relative strengths of the molecular forces that dictate the observed RNA affinities and specificities of the aminoglycosides. On a practical level, thermodynamic data are required to establish a database that can be used to predict, over a range of conditions, the relative affinity of given aminoglycoside for a targeted RNA site (e.g., the A-site of 16S rRNA) versus binding to potential competing secondary sites (e.g., other looped and nonlooped duplex regions).

In this paper, we use a combination of spectroscopic and calorimetric techniques to characterize the binding of the three neomycin-class aminoglycosides shown in Figure 1 to

a RNA oligonucleotide (schematically depicted in Figure 2) that models the A-site of *E. coli* 16S rRNA. Our results provide insight into the thermodynamic driving forces that govern aminoglycoside recognition of the 16S rRNA A-site, while also revealing the thermodynamic impact that modifications of drug rings II and IV have on this recognition.

MATERIALS AND METHODS

RNA and Drug Molecules. The 27-mer RNA oligonucleotide used in this study was obtained in its PAGE-purified sodium salt form from Dharmacon Research, Inc. (Lafayette, CO). Neomycin trisulfate trihydrate and paromomycin sulfate were obtained from Fluka, while ribostamycin sulfate dihydrate was obtained from Sigma.

UV Spectrophotometry. All UV absorbance experiments were conducted on an AVIV Model 14DS Spectrophotometer (Aviv Associates; Lakewood, NJ) equipped with a thermoelectrically controlled cell holder. A quartz cell with a 1 cm path length was used for all the absorbance studies. Absorbance versus temperature profiles were measured at 274 nm with a 10 s averaging time. The temperature was raised in 0.5 °C increments, and the samples were allowed to equilibrate for 1 min at each temperature setting. In these thermal denaturation studies, the RNA solutions were 2 μM in strand and contained aminoglycoside at concentrations ranging from 0 to 8 μM. The buffer solutions for the UV melting experiments contained 10 mM sodium cacodylate (8.5 mM Na^+), 0.1 mM EDTA, and NaCl at concentrations ranging from 51.5 to 138.5 mM. The pH values of the experimental buffer solutions ranged from 5.5 to 7.0 and were adjusted, when necessary, by addition of 1 N HCl. For each optically detected transition, the melting temperature (T_m) was determined as previously described (*12*).

Isothermal Titration Calorimetry (ITC). Isothermal calorimetric measurements were performed at either 25 or 37 °C on a MicroCal VP-ITC (MicroCal, Inc.; Northampton, MA). In a typical experiment, 5 μL aliquots of 250 μM aminoglycoside were injected from a 250 μL rotating syringe (430 rpm) into an isothermal sample chamber containing 1.42 mL of a RNA solution that was 10 μM in strand. Each experiment of this type was accompanied by the corresponding control experiment in which 5 μL aliquots of 250 μM drug were injected into a solution of buffer alone. The duration of each injection was 5.0 s, and the delay between injections was 240 s. The initial delay prior to the first injection was 60 s. Each injection generated a heat burst curve (microcalories per second vs seconds). The area under each curve was determined by integration [using the Origin version 5.0 software (MicroCal, Inc.; Northampton, MA)] to obtain a measure of the heat associated with that injection. The heat associated with each drug-buffer injection was subtracted from the corresponding heat associated with each drug−RNA injection to yield the heat of drug binding for that injection. The buffer solutions for the ITC experiments contained either 10 mM sodium cacodylate, 10 mM ^{1}MES, or 10 mM ^{1}MOPS, as well as 0.1 mM EDTA. In addition, each solution contained sufficient NaCl to bring the total Na^+ concentration to 60 mM. The pH values of the ITC experimental solutions ranged from 5.5 to 7.0.

Differential Scanning Calorimetry (DSC). Heat capacity (ΔC_p) versus temperature (T) profiles for the thermally induced transition of the drug-free A-site RNA model duplex was measured using a Model 6100 Nano II Differential Scanning Calorimeter (Calorimetry Sciences Corp.; Provo, UT). The heating rate was 1 °C/min. The duplex transition enthalpy (ΔH_{Dup}) was calculated from the area under the heat capacity curve using the Origin version 5.0 software (MicroCal, Inc.; Northampton, MA). The RNA solutions were 40 μM in strand, and the buffer solutions contained 10 mM sodium cacodylate (pH 6.0), 51.5 mM NaCl, and 0.1 mM EDTA.

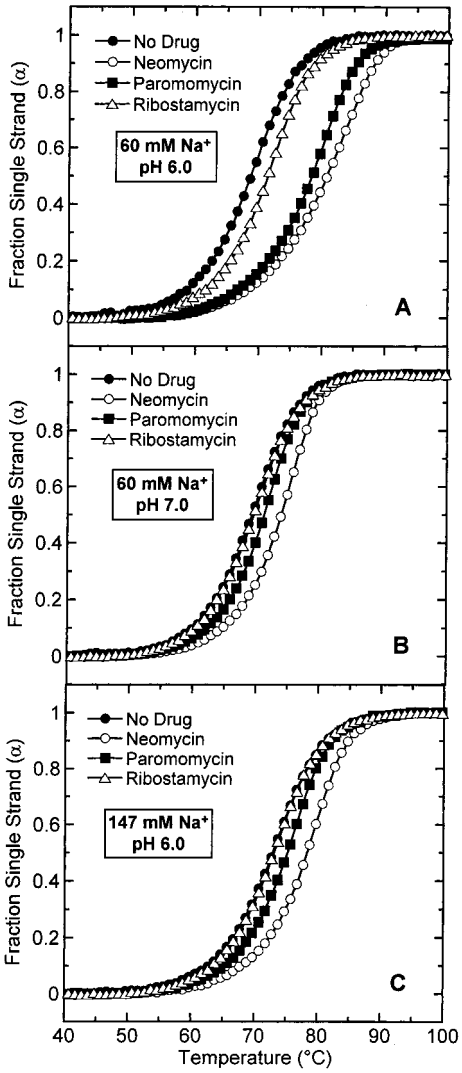

FIGURE 3: UV melting profiles for the A-site RNA oligonucleotide and its aminoglycoside complexes at a [drug]/[RNA] ratio (r_{RNA}) of 1.0. The Na^+ concentrations and pH values are as indicated. For clarity of presentation, the melting curves were normalized by subtraction of the upper and lower baselines to yield plots of fraction single strand (α) vs temperature (*12*). All the UV melting profiles were acquired at 274 nm.

RESULTS AND DISCUSSION

Neomycin, Paromomycin, and Ribostamycin Bind to and Enhance the Thermal Stability of the A-Site RNA Oligonucleotide in a Manner That Is Sensitive to Both pH and Na^+ Concentration. Figure 3A shows the UV melting curves for the A-site hairpin oligonucleotide duplex in the absence and presence of neomycin, paromomycin, or ribostamycin at a drug-to-RNA ratio (r_{RNA}) of 1.0. Note that at pH 6.0

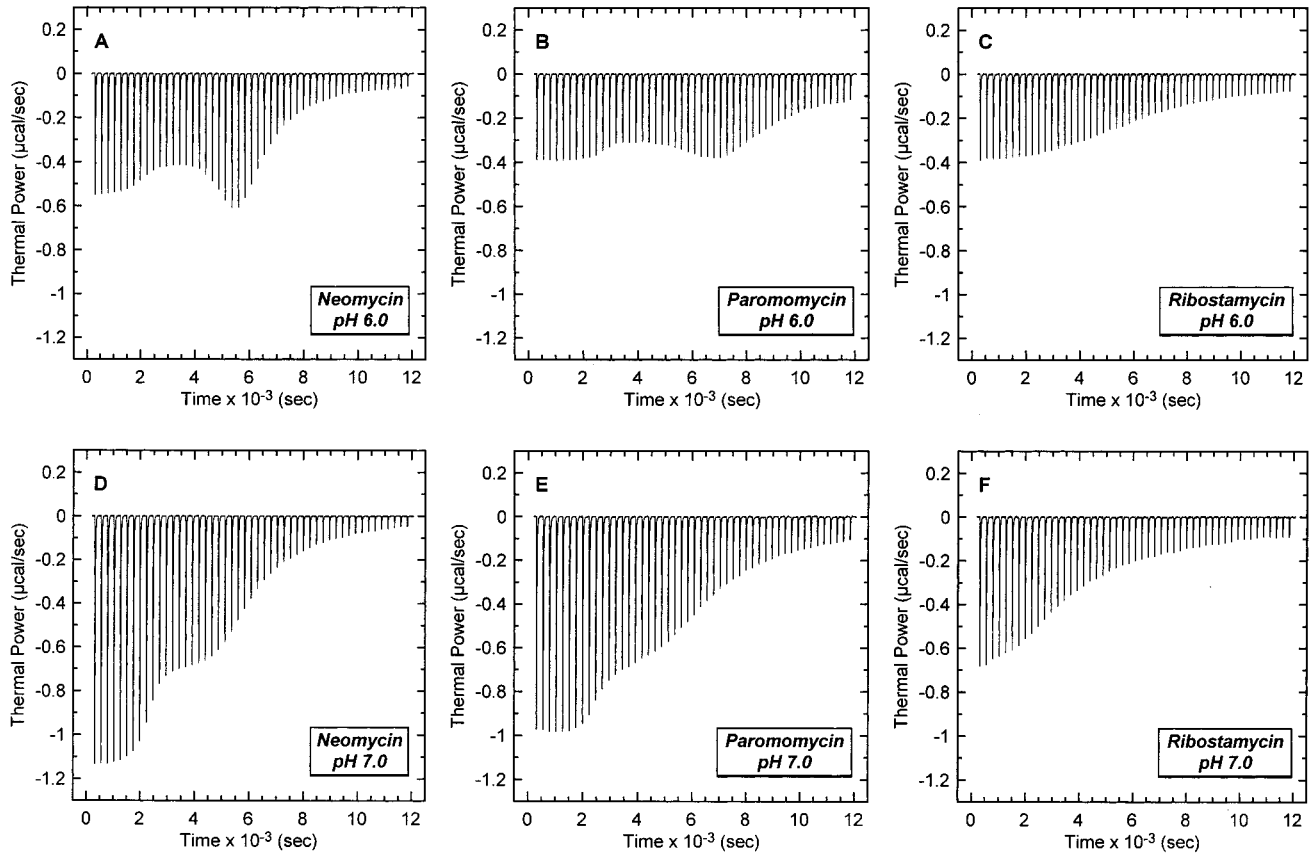

FIGURE 4: ITC profiles at 25 °C for the titration of either neomycin (A, D), paromomycin (B, E), or ribostamycin (C, F) into a solution of the A-site RNA oligonucleotide at pH 6.0 (A−C) or 7.0 (D−F). Each heat burst curve is the result of a 5 μL injection of 250 μM drug. The RNA concentration was 10 μM in strand, and the solution conditions were 10 mM sodium cacodylate, 51.5 mM NaCl, and 0.1 mM EDTA.

and a Na^+ concentration of 60 mM, the presence of each aminoglycoside enhances the thermal stability (T_m) of the target RNA duplex. Further note that the extent of drug-induced enhancement in duplex thermal stability follows the hierarchy neomycin > paromomycin > ribostamycin. Specifically, the binding of neomycin, paromomycin, and ribostamycin increases the thermal stability of the host RNA duplex by 12.0, 9.7, and 2.7 °C, respectively. Higher r_{RNA} ratios than 1.0 result in only marginal increases in the T_m of the host RNA duplex, an observation indicative of secondary binding to the host duplex at high drug concentrations. In fact, our ITC studies detailed below reveal an overall binding stoichiometry of three drug molecules per duplex, with the exception of ribostamycin−RNA complexation at pH 7.0, which is associated with a binding stoichiometry of only two drug molecules per duplex.

The drug-induced enhancement in duplex thermal stability noted above is consistent with the aminoglycosides binding to the host RNA duplex, with a preference for the double-stranded versus the single-stranded state (*13*, *14*). The extent of this thermal enhancement (ΔT_m) is sensitive to both pH and Na^+ concentration. For example, at a constant Na^+ concentration of 60 mM, raising the pH from 6.0 to 7.0 decreases the drug-induced ΔT_m from 12.0 to 4.6 °C for neomycin, from 9.7 to 2.0 °C for paromomycin, and from 2.7 to 0.3 °C for ribostamycin (compare Figure 3A,B). Similarly, at a constant pH of 6.0, raising the Na^+ concentration from 60 to 147 mM decreases the drug-induced ΔT_m from 12.0 to 5.4 °C for neomycin, from 9.7 to 2.3 °C for paromomycin, and from 2.7 to 0.2 °C for ribostamycin (compare Figure 3A,C). Thus, the extent to which binding by the aminoglycosides thermally stabilizes the host RNA duplex decreases with increasing pH and/or Na^+ concentration. This Na^+ and pH dependence of ΔT_m is consistent with at least one drug NH_3^+ group playing an important role in the binding of the aminoglycosides to the host RNA duplex.

Thermodynamics of Aminoglycoside Binding to the A-Site Oligonucleotide, as Determined Using Isothermal Titration Calorimetry: The Binding Enthalpy Becomes Increasingly Exothermic with Increasing pH. We used isothermal titration calorimetry (ITC) to characterize the binding of neomycin, paromomycin, and ribostamycin to the A-site oligonucleotide in cacodylate buffer at a constant Na^+ concentration of 60 mM and different values of pH. Figure 4 shows representative ITC profiles resulting from the injection of neomycin (panels A and D), paromomycin (panels B and E), or ribostamycin (panels C and F) into a solution of A-site RNA oligonucleotide at pH 6.0 (panels A−C) or 7.0 (panels D−F). Each of the heat burst curves in Figure 4 corresponds to a single drug injection. The areas under these heat burst curves were determined by integration to yield the associated injection heats. These injection heats were corrected by subtraction of the corresponding dilution heats derived from the injection of identical amounts of drug into buffer alone. Figure 5 shows the resulting corrected injection heats plotted as a function of the [drug]/[duplex] ratio. In this figure, the data points reflect the experimental injection heats, while the solid lines, when present, reflect the calculated fits of

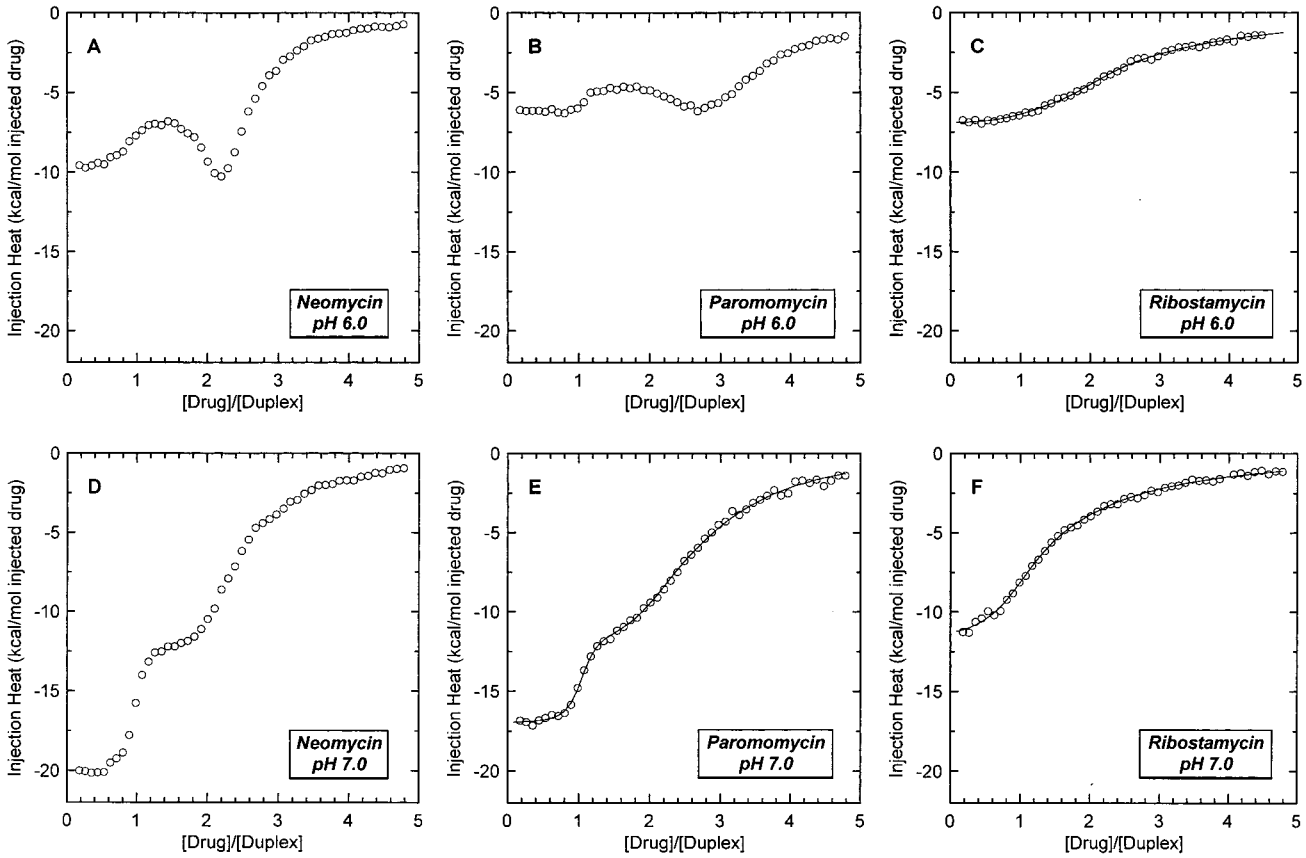

FIGURE 5: Corrected injection heats plotted as a function of the [drug]/[RNA] ratio. The corrected injection heats were derived by integration of the ITC profiles shown in Figure 4, followed by subtraction of the corresponding dilution heats derived from control titrations of drug into buffer alone. The data points reflect the experimental injection heats, while the solid lines in panels C, E, and F reflect calculated fits of the data. The data in panels C and E were fit with a model for three sequential binding sites, while the data in panel F were fit with a model for two sequential binding sites.

the data. The injection heat data corresponding to the titration of the RNA oligonucleotide with ribostamycin at pH 6.0 (Figure 5C) and paromomycin at pH 7.0 (Figure 5E) were fit with a model for three sequential binding sites. By contrast, the injection heat data corresponding to the titration of the RNA oligonucleotide with ribostamycin at pH 7.0 (Figure 5F) were fit with a model for two sequential binding sites. Thus, a pH increase from 6.0 to 7.0 reduces the overall binding stoichiometry of ribostamycin from three to two drug molecules per duplex. For each of the ITC titrations shown in Figure 5C,E,F, the model employed was the only model that yielded a reasonable fit of the experimental data. Note that the injection heat data corresponding to the titration of the RNA oligonucleotide with neomycin and paromomycin at pH 6.0 (Figure 5A,B), as well as the data corresponding to the titration of the RNA oligonucleotide with neomycin at pH 7.0 (Figure 5D), could not be accurately fit with any model. Each of these ITC profiles has three apparent phases, suggestive of three distinct binding events. However, in each case, the steepness of the first of the three phases, which is indicative of a tight binding interaction (i.e., with an association constant, $K_a \geq 10^9$ M^{-1}), precluded us from accurately fitting the entire profile to obtain estimates of binding affinity and stoichiometry (N). Note that even the fit of the ITC profile for the binding of paromomycin to the host RNA at pH 7.0 (Figure 5E) yielded an association constant for the first binding event (K_1) of 2.7×10^8 M^{-1}, a value approaching the upper limit for accurately fitting ITC data. Despite not being able to fit the ITC profiles in Figure 5A,B,D, we were able to derive the binding enthalpy (ΔH_1) associated with the first apparent binding event exhibited in each profile by averaging the corrected injection heats for the first 5−9 injections. The fits of the ITC profiles shown in Figure 5C,E,F were derived using ΔH and K_a as free-floating parameters. Armed with the resulting values of K_a, we calculated the corresponding binding free energies (ΔG) using the following standard relationship:

$$\Delta G = -RT \ln(K_a) \quad (1)$$

These binding free energies, coupled with the binding enthalpies derived from the fitted ITC data, allowed us to calculate the corresponding entropic contributions to binding ($T\Delta S$; where ΔS is the binding entropy) using the standard relationship

$$T\Delta S = \Delta H - \Delta G \quad (2)$$

These analyses allowed us to derive the thermodynamic binding profiles summarized in Table 1. Inspection of the data in Table 1 reveals two features worthy of note:

(i) At pH 6.0, the first ribostamycin molecule binds to the host RNA with a 17-fold higher affinity than the second drug molecule and with a 472-fold higher affinity than the third drug molecule. Similarly, at pH 7.0, the first ribostamycin molecule binds to the host RNA with a 29-fold higher affinity than the second drug molecule. Like ribostamycin, the first

Table 1: ITC-Derived Thermodynamic Profiles for the Binding of Neomycin-Class Aminoglycosides to the A-Site Model RNA Oligonucleotide at 25 °C and a Na^+ Concentration of 60 mM[a]

	pH 6.0			pH 7.0		
binding parameter[b]	neomycin[c]	paromomycin[c]	ribostamycin[d]	neomycin[c]	paromomycin[d]	ribostamycin[e]
K_1 (M^{-1})	ND	ND	$(1.7 \pm 0.3) \times 10^7$	ND	$(2.7 \pm 0.5) \times 10^8$	$(1.6 \pm 0.2) \times 10^6$
ΔH_1 (kcal/mol)	-9.6 ± 0.1	-6.1 ± 0.1	-6.9 ± 0.1	-20.0 ± 0.1	-17.0 ± 0.1	-12.0 ± 0.2
$T\Delta S_1$ (kcal/mol)	ND	ND	$+3.0 \pm 0.2$	ND	-5.5 ± 0.2	-3.5 ± 0.3
ΔG_1 (kcal/mol)	ND	ND	-9.9 ± 0.1	ND	-11.5 ± 0.1	-8.5 ± 0.1
K_2 (M^{-1})	ND	ND	$(1.0 \pm 0.1) \times 10^6$	ND	$(3.2 \pm 0.5) \times 10^6$	$(5.5 \pm 0.3) \times 10^4$
ΔH_2 (kcal/mol)	ND	ND	-6.5 ± 0.2	ND	-11.9 ± 0.2	-15.7 ± 0.4
$T\Delta S_2$ (kcal/mol)	ND	ND	$+1.7 \pm 0.3$	ND	-3.0 ± 0.3	-9.2 ± 0.5
ΔG_2 (kcal/mol)	ND	ND	-8.2 ± 0.1	ND	-8.9 ± 0.1	-6.5 ± 0.1
K_3 (M^{-1})	ND	ND	$(3.6 \pm 0.3) \times 10^4$	ND	$(1.4 \pm 0.1) \times 10^5$	NA
ΔH_3 (kcal/mol)	ND	ND	-13.6 ± 0.7	ND	-14.3 ± 0.3	NA
$T\Delta S_3$ (kcal/mol)	ND	ND	-7.4 ± 0.8	ND	-7.3 ± 0.4	NA
ΔG_3 (kcal/mol)	ND	ND	-6.2 ± 0.1	ND	-7.0 ± 0.1	NA

[a] All the data in this table are derived from ITC experiments conducted in cacodylate buffer. [b] Unless otherwise indicated, values of K and ΔH were determined from fits of the ITC profiles, with the indicated uncertainties reflecting the standard deviations of the experimental data from the fitted curves. Values of ΔG were determined using eq 1 in the text, with the indicated uncertainties reflecting the maximum errors as propagated through eq 1. Values of $T\Delta S$ were determined using eq 2, with the indicated uncertainties reflecting the maximum errors as propagated through eq 2. [c] ND denotes "not determinable," since the ITC profiles of neomycin at pH 6.0 and 7.0, as well as of paromomycin at pH 6.0, could not be fit accurately. In these three cases, the ΔH_1 values were determined by averaging the corrected injection heats for the first 5−9 injections. [d] The ITC profiles of ribostamycin at pH 6.0 and paromomycin at pH 7.0 were fit with a model for three sequential binding sites, which assumes a binding stoichiometry (N) of one drug per binding site. [e] The ITC profile of ribostamycin at pH 7.0 was fit with a model for two sequential binding sites, which also assumes an N of one drug per binding site. NA denotes "not applicable."

paromomycin molecule to bind the host RNA at pH 7.0 exhibits an 84-fold higher affinity than the second drug molecule and a 19,286-fold higher affinity than the third drug molecule. Recall that the ITC profiles shown in panels A (neomycin at pH 6.0), B (paromomycin at pH 6.0), and D (neomycin at pH 7.0) of Figure 5 could not be fit accurately due to the high-affinity nature (i.e., steepness) of the first apparent binding event. In the aggregate, these results indicate that the affinity with which the first drug molecule binds to the host RNA duplex is greater than the corresponding binding affinities of the second or third drug molecules. This observation suggests that the first drug molecule binds to a unique high-affinity site on the target RNA and, as such, is consistent with the NMR studies of the Puglisi group probing the interaction of paromomycin with the same RNA oligonucleotide studied here (*6*). Significantly, these NMR studies revealed that a one-to-one ratio of drug to RNA resulted in a complex in which a single drug molecule was bound to a distinct site on the RNA (a site schematically depicted in Figure 2).

(ii) The observed enthalpies for the RNA binding of the first molecules of neomycin, paromomycin, and ribostamycin are more exothermic (negative) at pH 7.0 than at pH 6.0. Specifically, ΔH_1 changes from −9.6 to −20.0 kcal/mol for the binding of neomycin, from −6.1 to −17.0 kcal/mol for the binding of paromomycin, and from −6.9 to −12.0 kcal/mol for the binding of ribostamycin. Hence, the enthalpy for the complexation of all three drugs with the host RNA becomes increasingly favorable with increasing pH. Note that the pK_a values of the neomycin NH_2 groups have been determined previously to range from 5.74 to 8.80 (see Figure 1) (*15*). It is reasonable to suggest that the similar pK_a values apply to the corresponding NH_2 groups of paromomycin and ribostamycin. Given these pK_a values, a pH change from 6.0 to 7.0 will reduce the extent to which neomycin, paromomycin, and ribostamycin are protonated, particularly the protonation states of the amino groups at the 3-, 2′-, and/or 2‴-positions. The protonation of an NH_2 group, such as the 2-NH_2 group on D-glucosamine, is a known exothermic reaction (*16*, *17*). Thus, it is likely that the pH dependence of the observed drug−RNA binding enthalpies noted above reflects exothermic contributions from binding induced protonation of one or more drug NH_2 groups. In fact, as discussed in the next section, the observed drug−RNA binding enthalpies at a given pH are dependent on the ionization heat of the buffer employed, with the nature of this dependence being indicative of binding-linked proton uptake.

At pH Values of 6.0 and 7.0, the Binding of the Neomycin-Class Aminoglycosides to the A-Site RNA Oligonucleotide Is Linked to the Uptake of Protons. We sought to determine whether the pH dependence of the observed aminoglycoside−RNA binding enthalpies described above reflects a linkage between drug binding and the release or uptake of protons. Toward this end, in addition to the ITC measurements described above, which were conducted in cacodylate buffer, we also conducted identical experiments in either MES (at pH 6.0) or MOPS (at pH 7.0) buffer. Both MES and MOPS have different heats of ionization (ΔH_{ion}) than cacodylate (see Table 2). Thus, if the pH dependence of the observed binding enthalpies (ΔH_{obs}) reflects binding-induced protonation of the drug, then the values of ΔH_{obs} at a given pH should vary with the buffer. Furthermore, the number of protons linked to binding at a specific pH (Δn), as well as the intrinsic binding enthalpy (ΔH_{int}), a value that differs from ΔH_{obs} in that it excludes enthalpic contributions from ionization of the buffer, can be determined by simultaneous solution of the following two equations (*18*):

$$\Delta H_{obs1} = \Delta H_{int} + \Delta H_{ion1}\Delta n \quad (3a)$$

$$\Delta H_{obs2} = \Delta H_{int} + \Delta H_{ion2}\Delta n \quad (3b)$$

In these equations, the numerical subscripts refer to the different buffers.

The number of linked protons and intrinsic enthalpies associated with the binding of each drug to the host RNA

Table 2: pH and Buffer Dependence of the Observed and Intrinsic Enthalpies, as Well as Of the Number of Linked Protons, for the Binding of Neomycin-Class Aminoglycosides to the A-Site Model RNA Oligonucleotide at a Na^+ Concentration of 60 mM

drug	pH	buffer (10mM)	ΔH_{ion}[a] (kcal/mol)	ΔH_{obs}[b] (kcal/mol)	ΔH_{int}[b] (kcal/mol)	Δn[b] (per drug)
neomycin	6.0	cacodylate	−0.47	−9.6 ± 0.1	−9.4 ± 0.1	0.36 ± 0.05
neomycin	6.0	MES	+3.71	−8.1 ± 0.1	−9.4 ± 0.1	0.36 ± 0.05
paromomycin	6.0	cacodylate	−0.47	−6.1 ± 0.1	−6.0 ± 0.1	0.26 ± 0.05
paromomycin	6.0	MES	+3.71	−5.0 ± 0.1	−6.0 ± 0.1	0.26 ± 0.05
ribostamycin	6.0	cacodylate	−0.47	−6.9 ± 0.1	−6.7 ± 0.1	0.43 ± 0.05
ribostamycin	6.0	MES	+3.71	−5.1 ± 0.1	−6.7 ± 0.1	0.43 ± 0.05
neomycin	7.0	cacodylate	−0.47	−20.0 ± 0.1	−19.3 ± 0.1	1.42 ± 0.05
neomycin	7.0	MOPS	+5.22	−11.9 ± 0.2	−19.3 ± 0.1	1.42 ± 0.05
paromomycin	7.0	cacodylate	−0.47	−17.0 ± 0.1	−16.3 ± 0.1	1.55 ± 0.05
paromomycin	7.0	MOPS	+5.22	−8.2 ± 0.2	−16.3 ± 0.1	1.55 ± 0.05
ribostamycin	7.0	cacodylate	−0.47	−12.0 ± 0.1	−11.5 ± 0.1	1.11 ± 0.04
ribostamycin	7.0	MOPS	+5.22	−5.7 ± 0.1	−11.5 ± 0.1	1.11 ± 0.04

[a] Ionization heats (ΔH_{ion}) at 25 °C for the indicated buffers were taken from (*19*) and Fukada and Takahashi (1987, unpublished results). [b] The number of binding-linked protons (Δn) and intrinsic binding enthalpies (ΔH_{int}) at 25 °C were calculated using eqs 3a and 3b, as well as the corresponding experimentally observed binding enthalpies (ΔH_{obs}).

(as calculated by solution of eqs 3a and 3b) are summarized in Table 2. Note that the values of ΔH_{obs} for cacodylate listed in Table 2 reflect the corresponding values of ΔH_1 listed in Table 1. Inspection of the data in Table 2 reveals that at pH values of 6.0 and 7.0, ΔH_{obs} varies with the buffer. Specifically, at either pH, ΔH_{obs} is more exothermic in cacodylate buffer than in either MES or MOPS. Given the values of ΔH_{ion} for cacodylate, MES, and MOPS at 25 °C (−0.47, +3.71, and +5.22 kcal/mol, respectively) (*19*), this observation indicates that aminoglycoside-RNA complexation is coupled to the uptake of protons (i.e., a positive value of Δn). Calculation of Δn at pH 6.0 using eqs 3a and 3b yields values of +0.36 ± 0.05, +0.26 ± 0.05, and +0.43 ± 0.05 for the RNA binding of neomycin, paromomycin, and ribostamycin, respectively. Recall that the 3-amino group on ring I of neomycin has been previously assigned a pK_a value of 5.74, with the remaining amino groups on the drug having pK_a values ≥ 7.55 (see Figure 1) (*15*). With the reasonable assumption that the corresponding amino groups of paromomycin and ribostamycin have similar pK_a values, our results suggest that the 3-amino group on ring I, which is common to all three aminoglycosides, is the amino group whose protonation is linked to drug−RNA binding at pH 6.0. With this assumption, our observed Δn values ranging from +0.26 to +0.43 for drug−RNA complexation at pH 6.0 implies a pK_a value for the 3-amino group of the RNA-bound drug to be in the range of 6.12 to 6.45. In other words, RNA binding shifts the pK_a of the 3-amino group of ring I by approximately 0.38−0.71 units. Recent NMR and X-ray crystallographic studies on paromomycin in complex with different rRNA A-site constructs have revealed that the 3-amino group of ring I makes contact with a phosphate group on the RNA backbone (*6*, *11*, *20*). This interaction may account for the apparent RNA binding-induced shift that we observe in the pK_a of the 3-amino group.

Further inspection of the data in Table 2 reveals that the value of Δn associated with the RNA binding of all three aminoglycosides increases upon a pH change from 6.0 to 7.0. Specifically, raising the pH from 6.0 to 7.0 increases Δn from +0.36 ± 0.05 to +1.42 ± 0.05 for the binding of neomycin, from +0.26 ± 0.05 to +1.55 ± 0.05 for the binding of paromomycin, and from +0.43 ± 0.05 to + 1.11 ± 0.04 for the binding of ribostamycin. This result suggests that the protonation of at least one or more drug amino groups, in addition to the 3-amino group of ring I, is linked to RNA binding. One potential candidate for such an amino group is the 2′-amino group of ring II (which is common to all three drugs), since it has a reported pK_a value in neomycin of 7.55 (*15*) and would therefore be partially deprotonated at pH 7.0. Recently reported X-ray crystal (*20*) and NMR-derived (*6*) structures of paromomycin in complex with different A-site RNA oligonucleotides (including the RNA oligomer studied here) reveal that the 2′-amino group makes an intramolecular hydrogen bond with the 4″ ring oxygen atom of ring III, which has been postulated to be important for the drug to adopt the proper orientation for specific recognition of the RNA (*6*). This intramolecular interaction may be favored when the 2′-amino group is in its protonated state.

Note that the extent to which a pH change from 6.0 to 7.0 increases Δn ($\Delta\Delta n$) is greater for the binding of neomycin ($\Delta\Delta n = +1.06 \pm 0.10$) and paromomycin ($\Delta\Delta n = +1.29 \pm 0.10$) than for the binding of ribostamycin ($\Delta\Delta n = +0.68 \pm 0.09$). This observation suggests that at pH 7.0, the binding of neomycin and paromomycin to the host RNA may be coupled to the protonation of an amino group that ribostamycin lacks. Recall that ribostamycin lacks ring IV, which is present in both neomycin and paromomycin and contains amino groups at the 2‴- and 6‴-positions (see Figure 1). The reported pK_a values for these two amino groups in neomycin are 7.60 and 8.80, respectively (Figure 1) (*15*). Thus, between these two amino groups, only the 2‴-amino group will exhibit any significant degree of deprotonation at pH 7.0 and is therefore a likely candidate for another amino group (in addition to the 2′- and 3-amino groups discussed above) whose protonation is linked to the RNA binding of neomycin and paromomycin. Significantly, as noted above in connection with the 3-amino group of ring I, recently reported paromomycin−rRNA structures (*6*, *20*) reveal that the 2‴-amino group of ring IV makes contact with RNA backbone phosphate functionalities and, if protonated, is thus poised for electrostatic interactions with these anionic phosphate groups. Such interactions would favor the protonated form of the 2‴-amino group and may therefore result in a binding-induced increase of its pK_a value.

Another feature of interest in Table 2 is the values of ΔH_{int}, which are the true intrinsic drug−RNA binding enthalpies that are independent of the buffer system employed. Note

Table 3: Temperature Dependent Enthalpy and Corresponding Heat Capacity Changes for the Binding of Neomycin-Class Aminoglycosides to the A-Site Model RNA Oligonucleotide at a Na^+ Concentration of 60 mM[a]

drug	pH	ΔH_{obs} @ 25 °C (kcal/mol)	ΔH_{obs} @ 37 °C (kcal/mol)	ΔC_p[b] (cal mol^{-1} K^{-1})
neomycin	6.0	-9.6 ± 0.1	-14.5 ± 0.1	-408 ± 17
paromomycin	6.0	-6.1 ± 0.1	-10.3 ± 0.2	-350 ± 25
ribostamycin	6.0	-6.9 ± 0.1	-9.6 ± 0.1	-225 ± 17
neomycin	7.0	-20.0 ± 0.1	-25.8 ± 0.2	-483 ± 25
paromomycin	7.0	-17.0 ± 0.1	-22.7 ± 0.1	-475 ± 17
ribostamycin	7.0	-12.0 ± 0.1	-14.9 ± 0.2	-242 ± 25

[a] All the data in this table are derived from ITC experiments conducted in cacodylate buffer. [b] Heat capacity changes (ΔC_p) were determined using eq 4 and the observed enthalpy changes listed in columns 3 and 4. The indicated uncertainties reflect the maximum errors in the values of ΔH_{obs} as propagated through eq 4.

that while the absolute values of ΔH_{int} differ from the corresponding values of ΔH_{obs}, the patterns of pH and drug dependence of ΔH_{obs} described in the previous sections are maintained in ΔH_{int}.

Neomycin-Class Aminoglycoside Binding to the A-Site RNA Oligonucleotide Is Associated with a Negative Heat Capacity Change (ΔC_p), the Magnitude of Which Increases with Increasing pH. In addition to the ITC experiments described in the previous sections, which were all conducted at 25 °C, we also conducted parallel ITC experiments at 37 °C. The values of ΔH_{obs} derived from these ITC experiments conducted at two different temperatures enabled us to determine the heat capacity change (ΔC_p) associated with the aminoglycoside−RNA interactions using the following standard relationship:

$$\Delta C_p = \frac{\Delta H_{T_1} - \Delta H_{T_2}}{T_1 - T_2} \quad (4)$$

The resulting values of ΔH_{obs} [which reflect the observed enthalpies for the first binding event (i.e., ΔH_1)] and ΔC_p are listed in Table 3. Note that, at pH 6.0, the RNA binding of neomycin, paromomycin, and ribostamycin is associated with a negative ΔC_p, with the magnitudes of these values following the hierarchy neomycin (-408 cal mol^{-1} K^{-1}) > paromomycin (-350 cal mol^{-1} K^{-1}) > ribostamycin (-225 cal mol^{-1} K^{-1}). These negative ΔC_p values reflect contributions not only from the binding equilibrium between the drug and the host RNA, but also from the coupled protonation equilibrium. Further, note that the ΔC_p for the binding of the three drugs to the host RNA becomes even more negative with a pH change from 6.0 to 7.0. Specifically, increasing the pH from 6.0 to 7.0 changes the value of ΔC_p from -408 to -483 cal mol^{-1} K^{-1} for the binding of neomycin, from -350 to -475 cal mol^{-1} K^{-1} for the binding of paromomycin, and from -225 to -242 cal mol^{-1} K^{-1} for the binding of ribostamycin. Recall that a pH increase from 6.0 to 7.0 is associated with a corresponding increase in the number of protons that are taken up as a result of the RNA binding reaction (see Table 2). Hence, the pH-induced increase in the magnitude of ΔC_p ($\Delta\Delta C_p$) is likely to reflect contributions from the corresponding pH-induced enhancement in the extent of binding-linked drug protonation ($\Delta\Delta n$). In fact, $\Delta\Delta C_p$ and $\Delta\Delta n$ follow the same hierarchies (compare Tables 2 and 3); namely, paromomycin > neomycin > ribostamycin.

Reductions in solvent accessible surface are known to have an impact on the value of ΔC_p (*21*−*24*), with the burial of nonpolar surfaces causing ΔC_p values to be more negative and the burial of polar surfaces causing ΔC_p values to be more positive. Thus, it is likely that the negative ΔC_p values we observe accompanying aminoglycoside−RNA complexation include contributions from binding-induced reductions in nonpolar solvent accessible surface. In this connection, the paromomycin−rRNA structures recently reported by the Puglisi (*6*) and Westhof (*20*) groups reveal that ring II of the drug stacks with guanine 1491, whose base pair with cytosine 1409 forms the floor of the drug binding site. This interaction significantly reduces the nonpolar solvent accessible surface of ring II and is likely to contribute to the observed negative ΔC_p values associated with the RNA binding of all three aminoglycosides studied here. In addition, recall that at pH 6.0, the ΔC_p value for the binding of ribostamycin is significantly less negative than the corresponding ΔC_p values for the binding of neomycin and paromomycin, despite the three drugs exhibiting similar Δn values at this pH. Thus, the comparatively less negative ΔC_p value for the binding of ribostamycin versus those values for the binding of neomycin and paromomycin may be due to the absence of ring IV in ribostamycin, which, in turn, reduces the amount of nonpolar surface that can be buried upon RNA binding. Note that the magnitude and sign of the ΔC_p values we observe for aminoglycoside−RNA complexation fall within the range of -100 to -550 cal mol^{-1} K^{-1} that is typically observed for both ligand−nucleic acid as well as ligand−protein interactions (*23*−*27*).

Neomycin, Paromomycin, and Ribostamycin Exhibit Differential Affinities for the A-Site RNA Oligonucleotide. A comparison of the RNA binding affinities of neomycin, paromomycin, and ribostamycin offers us the opportunity to evaluate the impact of specific alterations in drug structure on RNA complexation. Recall that we were able to determine association constants for the RNA binding of paromomycin at pH 7.0, as well as for the RNA binding of ribostamycin at both pH 6.0 and 7.0, by fitting the ITC data shown in Figure 5C,E,F. Unfortunately, the tight binding of neomycin and paromomycin to the host RNA at pH 6.0, as well as of neomycin at pH 7.0, precluded us from accurately fitting the ITC profiles shown in Figure 5A,B,D. Thus, from these ITC profiles, we were able to determine only the observed binding enthalpies associated with the first apparent binding event (ΔH_1 in Table 1). To determine neomycin−RNA association constants at pH 6.0 and 7.0, as well as a paromomycin−RNA association constant at pH 6.0, we used the ΔT_m approach described below. The measured change in the thermal stability of the host RNA duplex induced by the drug under consideration (see Figure 3) was used to estimate the apparent drug−RNA association constant at T_m (K_{T_m}) from the following expression (*13*):

$$\frac{1}{T_{m0}} - \frac{1}{T_m} = \frac{NR}{\Delta H_{Dup}} \ln(1 + K_{T_m} L) \quad (5)$$

In this expression, T_{m0} and T_m are the melting temperatures of the drug-free and drug-bound duplex, respectively, N is the number of drug molecules bound per duplex, ΔH_{Dup} is the enthalpy change for the melting of the duplex in the absence of bound drug [a value we determined by differential

Table 4: pH Dependence of ΔT_m-Derived Association Constants at 25 °C for the Complexation of Neomycin-Class Aminoglycosides to the A-Site Model RNA Oligonucleotide at a Na^+ Concentration of 60 mM

drug	pH	T_{m0} (°C)[a]	T_m (°C)[a]	$K_{25}^{T_m}$ (M^{-1})[b]
neomycin	6.0	68.8	80.8	$(9.4 \pm 4.0) \times 10^9$
paromomycin	6.0	68.8	78.5	$(9.3 \pm 4.2) \times 10^8$
ribostamycin	6.0	68.8	71.5	$(2.0 \pm 0.6) \times 10^7$
neomycin	7.0	69.2	73.8	$(4.8 \pm 1.8) \times 10^9$
paromomycin	7.0	69.2	71.2	$(3.9 \pm 1.4) \times 10^8$
ribostamycin	7.0	69.2	69.5	$(3.2 \pm 4.0) \times 10^6$

[a] T_m values were derived from UV melting profiles of the A-site model oligonucleotide in the absence (T_{m0}) and presence of drugs (at a [total drug] to [RNA] ratio of 1.0), with an uncertainty in the data of ±0.1 °C. [b] Association constants at 25 °C ($K_{25}^{T_m}$) were determined using eqs 5 and 6 as described in the text. For application of eq 5, we used DSC to determine the requisite value of ΔH_{Dup} (+76.0 ± 2.5 kcal/mol). For application of eq 6, we used ITC to determine the requisite values of ΔH_{int} and ΔC_p listed in Tables 2 and 3, respectively.

scanning calorimetry (DSC) to be +76.0 ± 2.5 kcal/mol], and L is the free drug concentration at T_m (which can be estimated by one-half the total drug concentration). We then extrapolated this binding constant at T_m to a reference temperature of 25 °C ($K_{25}^{T_m}$) using the following relationship (*28*):

$$K_T = \frac{K_{T_m}}{e^{-\Delta H_T/R(1/T_m - 1/T)} e^{\Delta C_p T/R(1/T_m - 1/T)} \left(\frac{T_m}{T}\right)^{\Delta C_p/R}} \quad (6)$$

The resulting $K_{25}^{T_m}$ values for the RNA binding of all three drugs studied here at both pH 6.0 and 7.0 are listed in Table 4. Note that these $K_{25}^{T_m}$ values reflect the association constants of the first drug molecules to bind the host RNA (i.e., K_1 in Table 1). Inspection of the data in Table 4 reveals a number of significant features: (i) The $K_{25}^{T_m}$ values for ribostamycin−RNA complexation at both pH 6.0 [$(2.0 \pm 0.6) \times 10^7$ M^{-1}] and 7.0 [$(3.2 \pm 4.0) \times 10^6$ M^{-1}], as well as the $K_{25}^{T_m}$ value for paromomycin−RNA complexation at pH 7.0 [$(3.9 \pm 1.4) \times 10^8$ M^{-1}], are in excellent agreement with the corresponding K_1 values derived from fits of the ITC profiles shown in panels C [$(1.7 \pm 0.3) \times 10^7$ M^{-1}], F [$(1.6 \pm 0.2) \times 10^6$ M^{-1}], and E [$(2.7 \pm 0.5) \times 10^8$ M^{-1}] of Figure 5 (compare Tables 1 and 4). This gratifying concordance between association constants derived from two independent approaches validates our use of the ΔT_m method to calculate aminoglycoside−RNA association constants, particularly under conditions where tight drug−RNA binding precludes accurate fitting of ITC data. (ii) At pH 6.0, the affinity of neomycin for the host RNA is approximately 10-fold greater than the affinity of paromomycin, while being approximately 12-fold greater at pH 7.0. Thus, under the conditions employed, the presence of a 6′-amino versus a 6′-hydroxyl group (compare the structures of neomycin and paromomycin in Figure 1) enhances the affinity for the host RNA by roughly 1 order of magnitude. (iii) At pH 6.0, the affinity of neomycin for the host RNA is 470-fold greater than the affinity of ribostamycin, while being 1500-fold greater at pH 7.0. Hence, the presence of ring IV provides a substantial contribution to RNA binding affinity, the magnitude of which increases with increasing pH.

Thermodynamic Origins of the Differential Affinities Exhibited by Neomycin, Paromomycin, and Ribostamycin for the A-Site RNA Oligonucleotide. We supplemented the calorimetric data in Tables 1 and 2 with the appropriate $K_{25}^{T_m}$ data from Table 4 to derive complete thermodynamic profiles for the RNA binding of all three aminoglycosides studied here at pH 6.0 and 7.0. The resulting thermodynamic profiles are summarized in Table 5. Note that the thermodynamic parameters listed in Table 5 are intrinsic binding parameters and thus are independent of the buffer system employed. Inspection of the data in Table 5 reveals a number of features worthy of note:

(i) At both pH 6.0 and 7.0, the RNA binding affinities of the three aminoglycosides exhibit the following hierarchy: neomycin > paromomycin > ribostamycin. Note the agreement between this hierarchy and that described above for the binding-induced enhancement in duplex thermal stability (see Figure 3 and Table 4). Thus, in this case, the relative extent to which drug binding thermally stabilizes the target RNA is correlated with its relative binding affinity.

(ii) The affinities of all three drugs for the host RNA duplex decreases by 0.4−1.4 kcal/mol (depending on the drug) with a pH increase from 6.0 to 7.0. This decrease in affinity occurs despite a corresponding enhancement in binding enthalpy (ΔH_{int}) ranging from 4.8 to 10.3 kcal/mol. By contrast, the pH change from 6.0 to 7.0 reduces the entropic contribution to binding ($T\Delta S_{int}$) by 6.2−11.0 kcal/mol, depending on the drug. In fact, for each drug, $T\Delta S_{int}$ changes from a positive (favorable) value at pH 6.0 to a negative (unfavorable) value at pH 7.0. These pH-dependent changes in ΔH_{int} and $T\Delta S_{int}$ are consistent with the binding-induced protonation events discussed above, since such protonation events are enthalpically favorable, while being entropically costly. Note that the pH-induced gains in enthalpy only partially compensate the corresponding losses in binding entropy, thereby resulting in a net reduction in binding free energy (i.e., affinity), which is entirely entropic in origin. In other words, raising the pH lowers the RNA binding affinities of the drugs because the corresponding gain in binding enthalpy that accompanies binding-induced protonation is not sufficient to overcome the concomitant loss in binding entropy.

(iii) At pH 6.0, neomycin exhibits a 1.4 kcal/mol higher affinity for the host RNA than paromomycin and a 1.7 kcal/mol higher affinity at pH 7.0. In both cases, the reduced binding affinity of paromomycin relative to that of neomycin is the result of a less favorable binding enthalpy. In fact, relative to neomycin, the reduced affinity of paromomycin occurs despite an enhanced entropic contribution to binding, which cannot compensate the substantially less favorable binding enthalpy. Thus, the enhanced affinity of neomycin for the target duplex relative to that of paromomycin is entirely enthalpic in origin. Recall that neomycin and paromomycin differ with respect to the substituent at the 6′-position, with this substituent being an OH group in paromomycin and a NH_3^+ group in neomycin (see Figure 1). Hence, the presence of a 6′-NH_3^+ versus a 6′-OH group results in an enthalpically driven enhancement in affinity. Our buffer-dependent calorimetric data discussed above (see Table 2) reveal that both neomycin and paromomycin exhibit similar degrees of binding-induced protonation at pH 6.0 and 7.0. Furthermore, the 6′-NH_3^+ group of neomycin has a

Table 5: Thermodynamic Profiles for the Binding of Neomycin-Class Aminoglycosides to the A-Site Model RNA Oligonucleotide at 25 °C and a Na^+ Concentration of 60 mM

drug	pH	ΔH_{int}[a] (kcal/mol)	$T\Delta S_{int}$[a] (kcal/mol)	ΔG @ 25 °C[b] (kcal/mol)	K_a @ 25 °C (M^{-1})
neomycin	6.0	-9.4 ± 0.1	$+4.2 \pm 0.3$	-13.6 ± 0.2	$(9.4 \pm 4.0) \times 10^{9}$ [c]
paromomycin	6.0	-6.0 ± 0.1	$+6.2 \pm 0.3$	-12.2 ± 0.2	$(9.3 \pm 4.2) \times 10^{8}$ [c]
ribostamycin	6.0	-6.7 ± 0.1	$+3.2 \pm 0.2$	-9.9 ± 0.1	$(1.7 \pm 0.3) \times 10^{7}$ [d]
neomycin	7.0	-19.3 ± 0.1	-6.1 ± 0.3	-13.2 ± 0.2	$(4.8 \pm 1.8) \times 10^{9}$ [c]
paromomycin	7.0	-16.3 ± 0.1	-4.8 ± 0.2	-11.5 ± 0.1	$(2.7 \pm 0.5) \times 10^{8}$ [d]
ribostamycin	7.0	-11.5 ± 0.1	-3.0 ± 0.2	-8.5 ± 0.1	$(1.6 \pm 0.2) \times 10^{6}$ [d]

[a] ΔH_{int} and ΔS_{int} are the intrinsic binding enthalpy and entropy, respectively. These intrinsic binding parameters are independent of the buffer employed. Values of ΔH_{int} were determined as described in the text, while values of $T\Delta S_{int}$ were determined using eq 2. [b] ΔG is the binding free energy, as determined using eq 1. [c] Association constants for neomycin at pH 6.0 and 7.0, as well as for paromomycin at pH 6.0, were derived using the ΔT_m-based approach described in the text. [d] Association constants for ribostamycin at pH 6.0 and 7.0, as well as for paromomycin at pH 7.0, were derived from fits of the corresponding ITC profiles.

reported pK_a of 8.60 (*15*) and, therefore, would be essentially fully protonated at both pH 6.0 and 7.0. Thus, it is unlikely that the enthalpy-driven enhanced RNA binding affinity of neomycin relative to paromomycin reflects significant contributions from differences in binding-linked protonation. Instead, the molecular basis for this enthalpy-driven enhanced affinity may reflect contributions from a number of different potential sources, including differential hydrogen bonding interactions (which are typically manifested enthalpically) and differential hydration changes (which have both enthalpic and entropic effects). Note that our observed 1.4−1.7 kcal/mol enhanced affinity of neomycin relative to paromomycin for the A-site RNA oligomer are similar in magnitude to those recently reported based on computational (*29*) and surface plasmon resonance studies (*30*).

(iv) At pH 6.0, neomycin exhibits a 3.7 kcal/mol higher affinity for the host RNA than ribostamycin and a 4.7 kcal/mol higher affinity at pH 7.0. At pH 6.0, the enhanced affinity of neomycin is 73% enthalpic and 27% entropic in origin, while, at pH 7.0, the enhanced affinity of neomycin is entirely enthalpic in origin. At pH 6.0, the 3.7 kcal/mol enhanced affinity of neomycin relative to ribostamycin is not likely to include contributions from binding-induced drug protonation, since both the 2‴- and 6‴-NH_3^+ groups of ring IV (which neomycin possesses but ribostamycin lacks) are essentially fully protonated at this pH (given their reported (*15*) pK_a values of 7.60 and 8.80, respectively). In fact, our buffer-dependent calorimetric studies described above (see Table 2) are consistent with this notion in revealing that both neomycin and ribostamycin exhibit similar degrees of binding-induced protonation ($\Delta n = 0.36$ and 0.43, respectively) at pH 6.0. Thus, the enhanced affinity of neomycin versus ribostamycin probably reflects contributions from multiple other sources, including differential hydrogen bonding patterns, differential solvent and counterion uptake/release, differential electrostatic interactions, and differential changes in solvent accessible surface. In connection with differential hydrogen bonding interactions, crystallographic studies by Ramakrishnan and co-workers on paromomycin in complex with the 30S ribosomal subunit of *Thermus thermophilus* have shown that the 6‴-NH_3^+ and 3‴-OH functionalities of ring IV make contact with the phosphates of both G1405 and C1490 (the equivalent base to U1490 in the *E. coli* 30S ribosomal subunit) (*11*). Such contacts would be absent in the ribostamycin−RNA complex, thereby reducing the binding free energy of ribostamycin relative to neomycin. In connection with the differential uptake/release of solvent and counterions, crystallographic and computational studies have revealed the presence of coordinated water molecules and positively charged ions in the highly electronegative major grooves of A-form nucleic acid duplexes (*31*−*38*). Hence, the reduced entropic contribution to the RNA binding of ribostamycin relative to neomycin may reflect differing extents of binding-induced solvent and counterion release from the RNA major groove by the two drugs, with the larger and more positively charged neomycin molecule causing more extensive release of solvent molecules and counterions than ribostamycin. The larger size (by virtue of having ring IV) and more positively charged nature (by virtue of having two additional amino groups) of neomycin relative to ribostamycin would allow neomycin to exhibit a larger binding-induced change in solvent accessible surface as well as more extensive electrostatic interactions with the host RNA. In fact, our ΔC_p results discussed above, coupled with recently reported structural and computational studies (*6*, *11*, *20*, *29*), provide support for both of these possibilities.

At pH 7.0, all the potential factors discussed above that would serve to enhance the RNA binding affinity of neomycin relative to ribostamycin are still valid. However, our buffer-dependent calorimetric studies described above (Table 2) indicate that the differential affinities of neomycin and ribostamycin at pH 7.0 also reflect contributions from differential binding-induced protonation, with the Δn value for the binding of neomycin (1.42) being greater than the corresponding value (1.11) for the binding of ribostamycin. These contributions would serve to reduce the affinity of neomycin relative to ribostamycin for the host RNA and would also account for the 100% enthalpic origins of the enhanced neomycin RNA binding affinity at pH 7.0 relative to pH 6.0 (at which the enhanced neomycin affinity is only 73% enthalpic in origin). Thus, the observed 4.7 kcal/mol enhanced affinity of neomycin versus ribostamycin would be even greater if it were not for the partially compensating effects of the differential binding-induced protonation.

Salt Dependencies of the Neomycin and Paromomycin Binding Affinities for the A-Site RNA Oligonucleotide Are Consistent with at Least Three Drug NH_3^+ Groups Participating in Electrostatic Interactions with the Host RNA. We used the ΔT_m method described above to derive neomycin−RNA and paromomycin−RNA association constants at 25 °C and pH 6.0 over a range of Na^+ concentrations. The resulting $K_{25}^{T_m}$ values are listed in Table 6. Note that for each drug, $K_{25}^{T_m}$ decreases with increasing Na^+ concentration.

Table 6: Salt Dependence of the ΔT_m-Derived Association Constants at 25 °C for the Complexation of Neomycin and Paromomycin with the A-Site Model RNA Oligonucleotide at pH 6.0

$[Na^+]$ (mM)	T_{m0} (°C)[a]	T_m (°C)[a]	$K_{25}^{T_m}$ (M^{-1})[b]
		Neomycin	
60	68.8	80.8	$(9.4 \pm 4.0) \times 10^9$
81	70.2	80.7	$(5.6 \pm 2.2) \times 10^9$
109	71.5	79.6	$(2.1 \pm 0.8) \times 10^9$
129	72.4	78.7	$(1.0 \pm 0.3) \times 10^9$
147	72.9	78.3	$(7.1 \pm 2.4) \times 10^8$
		Paromomycin	
60	68.8	78.5	$(9.3 \pm 4.2) \times 10^8$
81	70.2	77.3	$(3.3 \pm 1.4) \times 10^8$
109	71.5	76.1	$(1.2 \pm 0.5) \times 10^8$
129	72.4	75.9	$(6.8 \pm 2.7) \times 10^7$
147	72.9	75.2	$(3.6 \pm 1.5) \times 10^7$

[a] T_m values were derived from UV melting profiles of the A-site model oligonucleotide in the absence (T_{m0}) and presence of drug (at a [total drug] to [RNA] ratio of 1.0), with an uncertainty in the data of ±0.1 °C. [b] Association constants at 25 °C ($K_{25}^{T_m}$) were determined as described in the text, with the indicated uncertainties reflecting the maximum errors as propagated through eqs 5 and 6.

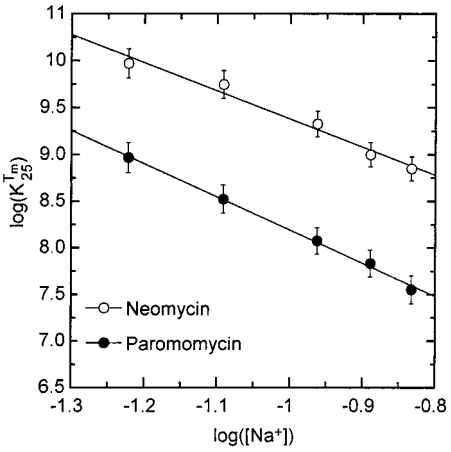

FIGURE 6: Salt dependence of the neomycin and paromomycin binding affinities for the A-site RNA oligonucleotide at pH 6.0. Log($K_{25}^{T_m}$) vs log([Na^+]) plots for neomycin (open circles) and paromomycin (filled circles) complexation with the host RNA. The experimental data points were fit by linear regression, with the resulting fits depicted as solid lines.

This observation indicates that electrostatic interactions play an important role in the binding of both drugs to the host RNA duplex. An estimate for the minimum number of drug NH_3^+ groups that participate in electrostatic interactions with the host RNA can be derived from plots of log($K_{25}^{T_m}$) versus log($[Na^+]$). Such plots for the data listed in Table 6 are shown in Figure 6. Note the linear dependencies of the data for both neomycin and paromomycin, which upon linear regression analyses, yield slopes $[(\partial \log K_{25}^{T_m})/(\partial \log [Na^+])]$ of -3.0 ± 0.4 and -3.6 ± 0.2, respectively, two values whose difference is within the experimental uncertainty. This observation is consistent with at least three drug NH_3^+ groups participating in electrostatic interactions with the RNA. Recall that the only difference between neomycin and paromomycin is that neomycin has an NH_3^+ group at the 6′-position of ring II instead of the OH group in paromomycin (see Figure 1). Further recall that the pK_a of the 6′-amino group of neomycin is 8.60 (*15*). Thus, at pH 6.0, the 6′-amino group of neomycin is essentially fully protonated, thereby affording neomycin one additional positive charge relative to paromomycin. Despite this additional charge, neomycin and paromomycin exhibit similar salt sensitivities in their binding to the host RNA. Thus, the enthalpy-driven enhanced RNA binding affinity of neomycin versus paromomycin afforded by the presence of the 6′-NH_3^+ group does not appear to reflect additional discrete electrostatic interactions in the neomycin−RNA complex.

CONCLUDING REMARKS

The studies reported here are minimum first steps toward establishing the thermodynamic database needed to provide insight into the molecular forces that dictate and control aminoglycoside recognition of RNA. Such a database will facilitate the rational design of aminoglycosides with predictable sequence- and/or structure-dependent RNA affinities and specificities. In this connection, specific alterations in rRNA sequence and structure have been shown to impart resistance to aminoglycoside activity (*39*, *40*), while others have been suggested as being the basis for the specificity of aminoglycosides for prokaryotic (versus eukaryotic) ribosomes (*41*, *42*). It has also been demonstrated that aminoglycoside targeting of specific RNA regions that serve as protein recognition sites interferes with protein binding and function (*43*−*49*). Thus, predictable binding affinities and specificities for predetermined RNA sites would have enormous value.

REFERENCES

1. Martin, A. R. (1998) in *Wilson and Gisvold's Textbook of Organic Medicinal and Pharmaceutical Chemistry* (Delgado, J. N., and Remers, W. A., Eds.) pp 253−325, Lippincott-Raven Publishers, Philadelphia.
2. Moazed, D., and Noller, H. F. (1987) *Nature 327*, 389−394.
3. Woodcock, J., Moazed, D., Cannon, M., Davies, J., and Noller, H. F. (1991) *EMBO J. 10*, 3099−3103.
4. Davies, J., Gorini, L., and Davis, B. D. (1965) *Mol. Pharmacol. 1*, 93−106.
5. Davies, J., and Davis, B. D. (1968) *J. Biol. Chem. 243*, 3312−3316.
6. Fourmy, D., Recht, M. I., Blanchard, S. C., and Puglisi, J. D. (1996) *Science 274*, 1367−1371.
7. Fourmy, D., Recht, M. I., and Puglisi, J. D. (1998) *J. Mol. Biol. 277*, 347−362.
8. Fourmy, D., Yoshizawa, S., and Puglisi, J. D. (1998) *J. Mol. Biol. 277*, 333−345.
9. Karimi, R., and Ehrenberg, M. (1994) *Eur. J. Biochem. 226*, 355−360.
10. Pape, T., Wintermeyer, W., and Rodnina, M. V. (2000) *Nat. Struct. Biol. 7*, 104−107.
11. Carter, A. P., Clemons, W. M., Brodersen, D. E., Morgan-Warren, R. J., Wimberly, B. T., and Ramakrishnan, V. (2000) *Nature 407*, 340−348.
12. Marky, L. A., and Breslauer, K. J. (1987) *Biopolymers 26*, 1601−1620.
13. Crothers, D. M. (1971) *Biopolymers 10*, 2147−2160.
14. McGhee, J. D. (1976) *Biopolymers 15*, 1345−1375.
15. Botto, R. E., and Coxon, B. (1983) *J. Am. Chem. Soc. 105*, 1021−1028.
16. Miyamoto, S., and Kazuko, M. (1958) *Kyoritsu Yakka Daigaku Kenkyû Nempô 4*, 12−16.
17. Tinoco, I., Jr., Sauer, K., and Wang, J. C. (1978) *Physical Chemistry: Principles and Applications in Biological Sciences*, Prentice-Hall, Englewood Cliffs.
18. Doyle, M. L., Louie, G., Dal Monte, P. R., and Sokoloski, T. D. (1995) *Methods Enzymol. 259*, 183−194.
19. Fukada, H., Takahashi, K., and Sturtevant, J. M. (1987) *Biochemistry 26*, 4063−4068.
20. Vicens, Q., and Westhof, E. (2001) *Structure 9*, 647−658.
21. Spolar, R. S., Livingstone, J. R., and Record, M. T. J. (1992) *Biochemistry 31*, 3947−3955.

22. Murphy, K. P., Xie, D., Garcia, K. C., Amzel, L. M., and Freire, E. (1993) *Proteins: Struct., Funct., Genet. 15*, 113−120.
23. Haq, I., Ladbury, J. E., Chowdhry, B. Z., Jenkins, T. C., and Chaires, J. B. (1997) *J. Mol. Biol. 271*, 244−257.
24. Mazur, S., Tanious, F. A., Ding, D., Kumar, A., Boykin, D. W., Simpson, I. J., Neidle, S., and Wilson, W. D. (2000) *J. Mol. Biol. 300*, 321−337.
25. Fisher, H. F., and Singh, N. (1995) *Methods Enzymol. 259*, 194−221.
26. Chaires, J. B. (1998) *Biopolym. Nucleic Acid Sci. 44*, 201−215.
27. Haq, I., Jenkins, T. C., Chowdhry, B. Z., Ren, J., and Chaires, J. B. (2000) *Methods Enzymol. 323*, 373−405.
28. Doyle, M. L., Brigham-Burke, M., Blackburn, M. N., Brooks, I. S., Smith, T. M., Newman, R., Reff, M., Stafford, W. F., III, Sweet, R. W., Truneh, A., Hensley, P., and O'Shannessy, D. J. (2000) *Methods Enzymol. 323*, 207−230.
29. Ma, C., Baker, N. A., Joseph, S., and McCammon, J. A. (2002) *J. Am. Chem. Soc. 124*, 1438−1442.
30. Alper, P. B., Hendrix, M., Sears, P., and Wong, C.-H. (1998) *J. Am. Chem. Soc. 120*, 1965−1978.
31. Gao, Y.-G., Robinson, H., van Boom, J. H., and Wang, A. H.-J. (1995) *Biophys. J. 69*, 559−568.
32. Cate, J. H., and Doudna, J. A. (1996) *Structure 4*, 1221−1229.
33. Adamiak, D. A., Milecki, J., Popenda, M., Adamiak, R. W., Dauter, Z., and Rypniewski, W. R. (1997) *Nucleic Acids Res. 25*, 4599−4607.
34. Sprous, D., Young, M. A., and Beveridge, D. L. (1998) *J. Phys. Chem. B 102*, 4658−4667.
35. Chin, K., Sharp, K. A., Honig, B., and Pyle, A. M. (1999) *Nat. Struct. Biol. 6*, 1055−1061.
36. Gao, Y.-G., Robinson, H. H., and Wang, A. H.-J. (1999) *Eur. J. Biochem. 261*, 413−420.
37. Misra, V. K., and Draper, D. E. (2000) *J. Mol. Biol. 299*, 813−825.
38. Misra, V. K., and Draper, D. E. (2001) *Proc. Natl. Acad. Sci. U.S.A.* 98, 12456−12461.
39. DeStasio, E. A., Moazed, D., Noller, H. F., and Dahlberg, A. E. (1989) *EMBO J. 8*, 1213−1216.
40. DeStasio, E. A., and Dahlberg, A. E. (1990) *J. Mol. Biol. 212*, 127−133.
41. Recht, M. I., Douthwaite, S., and Puglisi, J. D. (1999) *EMBO J. 18*, 3133−3138.
42. Lynch, S. R., and Puglisi, J. D. (2001) *J. Mol. Biol. 306*, 1037−1058.
43. Zapp, M. L., Stern, S., and Green, M. R. (1993) *Cell 74*, 969−978.
44. Zapp, M. L., Young, D. W., Kumar, A., Singh, R., Boykin, D. W., Wilson, W. D., and Green, M. R. (1997) *Bioorg. Med. Chem. 5*, 1149−1155.
45. Mei, H.-Y., Cui, M., Heldsinger, A., Lemrow, S. M., Loo, J. A., Sannes-Lowry, K. A., Sharmeen, L., and Czarnik, A. W. (1998) *Biochemistry 37*, 14204−14212.
46. Wang, S., Huber, P. W., Cui, M., Czarnik, A. W., and Mei, H.-Y. (1998) *Biochemistry 37*, 5549−5557.
47. Michael, K., and Tor, Y. (1998) *Chem. Eur. J. 4*, 2091−2098.
48. Tor, Y. (1999) *Angew. Chem., Int. Ed. Engl. 38*, 1579−1582.
49. Kirk, S. R., Luedtke, N. W., and Tor, Y. (2000) *J. Am. Chem. Soc. 122*, 980−981.
50. Recht, M. I., Fourmy, D., Blanchard, S. C., Dahlquist, K. D., and Puglisi, J. D. (1996) *J. Mol. Biol. 262*, 421−436.

BI020130F